New Intercalation Compounds of Layered Lanthanide Oxychlorides LnOCl (Ln = Ho, Er, Tm, and Yb) with Pyridine and Substituted Pyridines

Kang Song and Susan M. Kauzlarich*

Department of Chemistry, University of California, Davis, California 95616

Received August 20, 1993. Revised Manuscript Received February 8, 1994®

The lanthanide oxychlorides of Ho, Er, Tm, and Yb crystallize in the hexagonal space group, $R\bar{3}m$ as a mixture of the SmSI- and YOF-type layered structures. The oxychlorides are prepared by heating Ln_2O_3 (Ln = Ho, Er, Tm, and Yb) with excess NH_4Cl, followed by pyrohydrolysis. Crystalline phases of the lanthanide oxychlorides are obtained by heating LnOCl in LiCl/KCl fluxes at 450 °C. The cell parameters obtained from X-ray powder diffraction are as follows: HoOCl, a = 3.7697 (7), c = 27.766 (6) Å; ErOCl, a = 3.745 (1), c = 27.719 (8) Å; TmOCl, a = 3.708 (2), c = 27.72 (1) Å; YbOCl, a = 3.704 (2), c = 27.68 (2) Å. A series of new pyridine intercalation compounds, $(py)_x$LnOCl, have been prepared by reactions of pyridine with the LnOCl hosts. Intercalation compounds are characterized by X-ray powder diffraction, mass spectrometry, elemental analysis, thermal gravimetric analysis, infrared spectroscopy, and temperature-dependent magnetic susceptibility. There is no reduction of the host lattice and pyridine apparently intercalates as the neutral molecule. An acid–base interaction is proposed for the mode of intercalation of pyridine into the lanthanide oxychlorides. Further studies on the intercalation of substituted pyridines, 4-ethylpyridine, and 2,6-lutidine, indicate that the C_2 axis of pyridine is oriented perpendicular to the LnOCl layers.

Introduction

During the past two decades there has been a great deal of interest in the intercalation chemistry of Lewis bases with layered host materials, such as transition-metal dichalcogenides,[1-7] oxychlorides,[2,8-10] phosphorus trichalcogenides,[2,3,11,12] and oxide bronzes.[2,13-16] In these two dimensional solids, atoms are bound together by strong covalent or ionic forces within a layer, while distinct layers are held together by weak van der Waals forces. Weaker interlayer interactions offer the possibility of inserting guest species between the layers of these compounds. Although intercalation chemistry of layered transition metal compounds with Lewis bases such as ammonia and pyridine has been extensively studied, little attention has been given to the intercalation of Lewis bases into layered lanthanide compounds. The interest in studying lanthanide compounds stems from their potential electronic, magnetic, optical, and catalytic properties.[17] The majority of the LnOCl (Ln = lanthanide) compounds crystallize in the three-dimensional PbFCl structure and are not amenable to intercalation, while the heavier lanthanide oxychlorides are polymorphic and can also crystallize in the two-dimensional SmSI or YOF structure. Investigation of new intercalation compounds of the layered lanthanide oxychlorides LnOCl (Ln = Ho, Er, Tm, and Yb) has become possible since the successful synthesis of these compounds by low-temperature routes.[18] All of the four-layered lanthanide oxychlorides are isostructural and crystallize in the hexagonal space group $R\bar{3}m$. Their pyridine intercalation compounds are expected to exhibit similar physical and chemical properties. Intercalation of sodium[19] and pyridine[20] into YbOCl has been demonstrated. In this paper the synthesis of the LnOCl and their intercalation compounds with pyridine and substituted pyridines and the characterization of these new compounds by X-ray powder diffraction, mass spectrometry, elemental analysis, thermal gravimetric analysis, infrared spectroscopy, and temperature-dependent magnetic susceptibility will be presented in detail. The mechanism of intercalation reaction and the orientation of pyridine between the host layers will be discussed.

® Abstract published in *Advance ACS Abstracts,* March 15, 1994.

(1) *Intercalated Layered Materials: Physics and Chemistry of Materials with Layered Structures*; Lévy, F. A., Ed.; D. Reidel: Dordrecht, 1979; Vol. 6.
(2) *Intercalation Chemistry*; Whittingham, M. S., Jacobson, A. J., Eds.; Academic Press: New York, 1982.
(3) *Intercalation in Layered Materials*; Dresselhaus, M. S., Ed.; Plenum Press: New York, 1986; Vol. 148.
(4) Gamble, F. R.; Osiecki, J. H.; Disalvo, F. J. *J. Chem. Phys.* **1971**, *55*, 3525.
(5) Gamble, F. R.; Osieck, J. H.; Cais, M.; Pisharody, R. *Science* **1971**, *174*, 493.
(6) Schöllhorn, R. *Angew. Chem., Int. Ed. Engl.* **1980**, *19*, 983.
(7) Brec, R. *Solid State Ionics* **1986**, *22*, 3.
(8) Kikkawa, S.; Kanamaru, F.; Koizumi, M. *Bull. Chem. Soc. Jpn.* **1979**, *52*, 963.
(9) Herber, R. H.; Maeda, Y. *Inorg. Chem.* **1981**, *20*, 1409.
(10) Salmon, A.; Eckert, H.; Herber, R. H. *J. Chem. Phys.* **1984**, *81*, 5206.
(11) Joy, P. A.; Vasudevan, S. *J. Am. Chem. Soc.* **1992**, *114*, 7792.
(12) Clement, R.; Lomas, L.; Audiere, J. P. *Chem. Mater.* **1990**, *2*, 641.
(13) Schöllhorn, R.; Schulte-Nölle, T.; Steinhoff, G. *J. Less Common Met.* **1980**, *71*, 71.
(14) Johnson, J. W.; Jacobson, A. J.; Rich, S. M.; Brody, J. F. *J. Am. Chem. Soc.* **1981**, *103*, 5246.
(15) Dickens, P. G.; Hibble, S. J. *J. Solid State. Chem.* **1986**, *63*, 166.
(16) Savariault, J.-M.; Lafargue, D.; Parize, J.-L.; Galy, J. *J. Solid State Chem.* **1992**, *97*, 169.
(17) *New Frontiers in Rare Earth Science and Application*; Guangian, X., Jimei, X., Eds.; Academic Press: New York, 1985; Vols. I, II.
(18) Garcia, E.; Corbett, J. D.; Ford, J. E.; Vary, W. J. *Inorg. Chem.* **1985**, *24*, 494.
(19) Odink, D. A.; Kauzlarich, S. M. *Mol. Cryst. Liq. Cryst.* **1990**, *181*, 325.
(20) Odink, D. A.; Song, K.; Kauzlarich, S. M. *Chem. Mater.* **1992**, *4*, 906.

0897-4756/94/2806-0386$04.50/0

Experimental Section

Materials. Ln_2O_3 (Ln = Ho, Er, Tm, and Yb), 99.999%, was purchased from Research Chemicals. Anhydrous pyridine and substituted pyridines, 4-ethylpyridine and 2,6-lutidine (Aldrich), were obtained by drying the solvents over KOH pellets and then distilling from CaH_2. All purified solvents were stored over 4-Å molecular sieves and degassed prior to use. The salts, LiCl (anhydrous, 99.6%, AESAR) and KCl (Fisher), were dried overnight under vacuum (10^{-6} Torr) at 400 and 500 °C, respectively. KBr (99+%, FT-IR grade, Aldrich) was dried at 200 °C for several hours under vacuum and stored in a drybox.

Synthesis. LnOCl (Ln = Ho, Er, Tm, and Yb) is prepared by reaction of Ln_2O_3 with a 20% molar excess of NH_4Cl in two steps as shown below:[18]

$$Ln_2O_3 + 12NH_4Cl \rightarrow 2(NH_4)_3LnCl_6 + 6NH_3 + 3H_2O \quad (1)$$

$$(NH_4)_3LnCl_6 + H_2O \rightarrow LnOCl\ (R\bar{3}m) + 3NH_4Cl + 2HCl \quad (2)$$

Ln_2O_3 and NH_4Cl were mixed together and placed in a quartz tube (16-cm length and 2-cm diameter) with two narrowed ends. The quartz tube was then placed in a Pyrex tube that was long enough to extend from two sides of a vertical furnace. The first reaction was heated slowly to 270 °C for 1–2 days until NH_3 gas no longer evolved. The following hydrolysis of intermediate product $(NH_4)_3LnCl_6$ was carried out under Ar gas saturated with H_2O at 300 °C for ~10 days until HCl gas is no longer present, as indicated by a litmus test. Typically, 4 g of the LnOCl product were prepared in this manner. The products are mixed phases containing the SmSI and YOF structures that both belong to the $R\bar{3}m$ space group. They are not very crystalline and show only a few relatively broad lines that can be indexed in the $R\bar{3}m$ space group. However, these $R\bar{3}m$ disordered phases can be converted into more crystalline phases by a LiCl–KCl flux at 450 °C (LnOCl:LiCl/KCl = 1:20). The mixture of LnOCl (disordered) and LiCl/KCl salts (molar ratio of salts: 58.5/41.5) in an evacuated sealed quartz ampule was heated slowly to 450 °C for 20 days and then cooled quickly to room temperature. The product, LnOCl (crystalline), was separated from the salts by dissolving the flux in water, filtering out the salt solution, and rinsing the product with methanol. After being dried overnight in air, the crystalline LnOCl powder, less than 100 mesh, was selected and dried at 300 °C under high vacuum and characterized by X-ray powder diffraction, TGA, IR spectroscopy, and temperature-dependent magnetic susceptibility. Hydrogen content was determined by elemental analysis for one of the LnOCl products, YbOCl,[21] since the presence of interstitial hydrogen[22] or replacement of –Cl by –OH may be a concern. The hydrogen content was below detection levels (less than 0.1%) for the YbOCl sample.

Intercalation compounds of pyridine and substituted pyridines were prepared by immersing weighed solids of the LnOCl in pyridine or substituted pyridine solutions. Since all of the intercalates formed are moisture sensitive, they were handled under inert atmosphere at all times. The LnOCl material (150 mg) was placed into a sidearm flask in a nitrogen-filled drybox and then transferred to a Schlenck line. Anhydrous, degassed pyridine or substituted pyridine (20 mL) was injected into the flask with an oven-dried syringe. The flask was evacuated and sealed and the mixture was magnetically stirred at room temperature for 2 or 4 weeks. After 2 or 4 weeks, the excess solvent was removed. The product was dried under vacuum for several hours and then transferred into a drybox. The solids showed little or no change in color upon intercalation. The supernatant pyridine liquid also remained colorless after intercalation and showed only neutral pyridine in the IR, NMR, and MS. The intercalates were characterized by X-ray powder diffraction, mass spectrometry, elemental analysis,[21,23] thermal gravimetric analysis, IR spectroscopy, and temperature-dependent magnetic susceptibility.

X-ray Powder Diffraction. A Siemens X-ray powder diffractometer using Cu Kα radiation was used to obtain the data for the powder patterns shown in Figure 3 and for the lattice parameters of all the compounds prepared in this work. The air-sensitive sample was placed between two pieces of cellophane tape during measurement. A Guinier camera with Cu Kα_1 radiation was also used to facilitate identification of the samples. The sample was placed between two pieces of cellophane tape with about 10% NIST silicon for a standard. Sample integrity was maintained by dynamic vacuum.

TGA. Thermal gravimetric analysis was performed on a DuPont Model 951 thermogravimetric analyzer. All powder samples were pressed into pellets weighing between 10 and 20 mg, placed in platinum boats, and weight loss measured from 30 to 1000 °C with a heating rate of 5 °C/min under pure N_2 gas. The stoichiometries of intercalated pyridine (x) in the $(py)_xLnOCl$ compounds were obtained by calculating the weight difference between the pristine LnOCl and the pyridine intercalates between 200 and 300 °C, the temperature range at which the intercalated pyridine molecules withdraw completely from the host layers. The stoichiometries were confirmed by elemental analysis.[21,23] X-ray powder diffraction data of the product at 300 and 800 °C were taken immediately and the product identified.

Mass Spectrometry. Mass spectrometry (MS) was used to identify the gaseous species obtained from deintercalation and decomposition. The intercalates were heated from room temperature to 150 °C at a linear rate of 5 °C/min under vacuum (10^{-6} mbar). The evolved gases were detected using a Trio-2 mass spectrometer (VG Masslab, Altrincham, UK) operated at 70-eV electron ionization. Profiles of specific ion abundances were plotted to analyze the evolution of each of the gaseous species as a function of temperature. All samples showed only pyridine molecules as the gaseous species upon heating to 150 °C. All samples, except $(py)_{0.15}TmOCl$, showed only one peak in the temperature profile, indicative of one type of pyridine. The temperature profile for pyridine in $(py)_{0.15}TmOCl$ showed one peak with a small shoulder on the high-temperature side and may indicate two different interactions of the intercalated pyridine with the host. After complete deintercalation, the samples were further heated at a rate of 100 °C/min to 750 °C and HCl is observed as the only gaseous species.

IR Spectroscopy. Infrared spectra were recorded in the range 400–4000 cm^{-1} with a resolution of 2 cm^{-1} on an IR/32 IBM 9000 FTIR system. The sample was ground together with KBr and the mixture was pressed into a pellet attached on a sample holder. An equal mass of pure KBr pellet was used as the reference. All the measurements were carried out under flowing N_2 gas.

Magnetic Susceptibility. Temperature-dependent magnetic susceptibilities were measured on the Quantum Design SQUID magnetometer. Powder samples were pressed into pellets in a drybox, and small pieces of the broken pellets weighing between 10–20 mg were sealed into fused silica tubes under vacuum (10^{-6} Torr). The magnetic susceptibility data were collected between 10 and 300 K under magnetic fields of 2000 or 5000 G and fit to the Curie–Weiss law.

Results and Discussion

LnOCl. Figure 1 shows the local coordination of the oxychlorides in the SmSI structure.[24,25] Each Ln^{3+} ion is coordinated to four oxygen and three intralayer chlorine atoms. There are also three interlayer chlorine (Cl′ in Figure 1) ions that can be considered as next nearest neighbors at a much longer distance. In the YOF structure, the Ln^{3+} coordination differs only in the next nearest neighbor where there is only one interlayer chloride ion (Cl′) which caps the trigonal face formed by the three

(21) Berkeley Microanalytical Laboratory, University of California, 20 Lewis Hall, Berkeley, CA 94720.
(22) Meyer, G.; Hwu, S.; Wijeyesekera, S.; Corbett, J. D. *Inorg. Chem.* **1986**, *25*, 4811.
(23) Galbraith Laboratories, Inc., P.O. Box 51610, Knoxville, TN 27950.
(24) Brandt, G.; Diehl, R. *Mater. Res. Bull.* **1974**, *9*, 411.
(25) Beck, H. P. *Z. Naturforsch.* **1976**, *31b*, 1562.

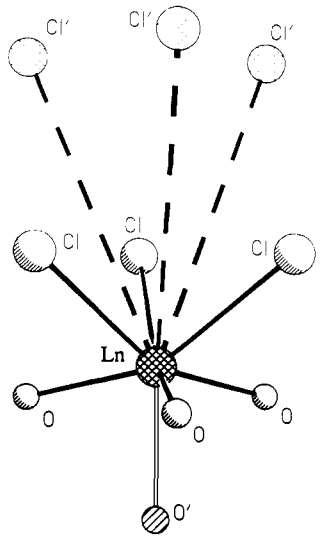

Figure 1. View of the coordination about Ln^{3+} in the SmSI structure of LnOCl.

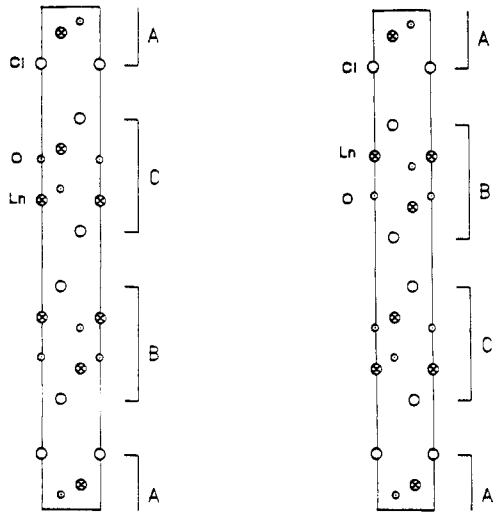

SmSI YOF

Figure 2. (110) projections of the stacking layers in the SmSI (ABC) and YOF (ACB) structures.

intralayer chlorines. The structure can be described as being formed from homoatomic layers, sequenced Cl–Ln–O–O–Ln–Cl.[18] The interlayer Cl–Cl′ distance of ~3.7 Å between the chloride planes is approximately twice as much as the Cl radius, indicating that the layers are held together by van der Waals forces. The difference in the next-nearest-neighbor coordination of the Ln^{3+} cation is the result of a difference in the stacking sequence of the layers. The difference in stacking sequence between the SmSI and YOF structures can be clearly seen in the (110) projections shown in Figure 2.

Although it has been reported that LiCl/KCl flux at low temperatures converts the LnOCl from the mixed structures into the SmSI structure,[18,20] LnOCl products obtained after the fluxes in this work were determined by X-ray powder diffraction to be still a mixture of the SmSI and YOF structures. The only distinguishing features of the two structures are the (101)–(012), (104)–(015), (018)–(107), and (1,0,10)–(0,1,11) reflections.[18] The calculated intensities[26] of YbOCl for the (101), (104), (018), and (1,0,-10) reflections are 32, 87, 36 and 16%, respectively, in the SmSI structure[24] and 1, 9, 1 and 9%, respectively, in the YOF structure.[18] In addition, the intensities for the (012), (015), (107), and (0,1,11) reflections are 0, 20, 3 and 0%, respectively, in the SmSI structure and 61, 57, 38 and 17%, respectively, in the YOF structure. Since all the LnOCl products obtained in this work show reflections from both structures, the flux appears to only increase the crystallinity of the product. The mixed phase (SmSI and YOF structures) obtained may be attributed to a larger quantity of material involved in the flux. The lattice parameters of these oxychlorides obtained from X-ray powder diffraction are listed in Table I and compared with literature values. Indexed powder diffraction patterns are available as supplementary material.

Table 1. Lattice Parameters for LnOCl Compounds Obtained from X-ray Powder Diffraction in Comparison with Literature Values

compound	structure type	a (Å)	c (Å)
HoOCl	SmSI + YOF	3.7697 (7)	27.766 (6)
	SmSI[a]	3.7681 (5)	27.70 (1)
	YOF[a]	3.7677 (4)	27.700 (5)
ErOCl	SmSI + YOF	3.745 (1)	27.719 (8)
	SmSI[a]	3.7462 (5)	27.63 (1)
	YOF[a]	3.7458 (6)	27.73 (1)
TmOCl	SmSI + YOF	3.708 (2)	27.72 (1)
	SmSI[a]	3.7425 (4)	27.852 (7)
	YOF[a]	3.730 (1)	27.74 (1)
YbOCl	SmSI + YOF	3.704 (2)	27.68 (2)
	SmSI[a]	3.700 (2)	27.76 (2)

[a] Powder diffraction data from ref 18.

Although the LnOCl compounds are not O_2 sensitive, they are hygroscopic. All investigations of intercalations discussed below are for the LnOCl obtained from the LiCl/KCl flux, 100 mesh, dried at 300 °C under vacuum (10^{-6} Torr). The samples were determined to be water free based on zero weight loss in the TGA and the absence of modes due to H_2O in the IR. Elemental analysis of YbOCl indicated that hydrogen content is less than 0.1%.[21]

$(py)_xLnOCl$. A series of new intercalation compounds is obtained by reactions of LnOCl with pyridine and substituted pyridines at room temperature for 2 or 4 weeks. A number of other experimental conditions have also been investigated[27] such as reaction temperature, presence of H_2O, and solvent effects. In all cases, some small amount of the LnOCl remains unintercalated, as indicated by the X-ray powder diffraction data shown in Figure 3. There is about 10% unintercalated LnOCl in the $(py)_xLnOCl$ based on a comparison of the intensities of the (*003*) reflections.

Table 2 shows the stoichiometries, lattice parameters, and interlayer spacing changes for the $(py)_xLnOCl$ compounds, prepared at room temperature for 2 or 4 weeks. Indexed X-ray powder diffraction patterns are provided as supplementary materials. Table 3 shows the calculated and experimental C, H, N analyses. Since there is about 10% unintercalated LnOCl in the sample, the actual x values for the samples are slightly higher than what is obtained from TG and elemental analyses. In the case of $(py)_xErOCl$ and $(py)_xYbOCl$ compounds, the content of intercalated pyridine (x) increases in the first 2 weeks and then shows little change up to 4 weeks. Higher temper-

(26) Clark, C. M.; Smith, D. K.; Johnson, G. J., *A Fortran IV Program for Calculating X-ray Powder Diffraction Patterns—Version 5*; Department of Geosciences, The Pennsylvania State University, University Park, PA, 1973.

(27) Song, K.; Kauzlarich, S. M. *J. Alloys Compounds*, in press.

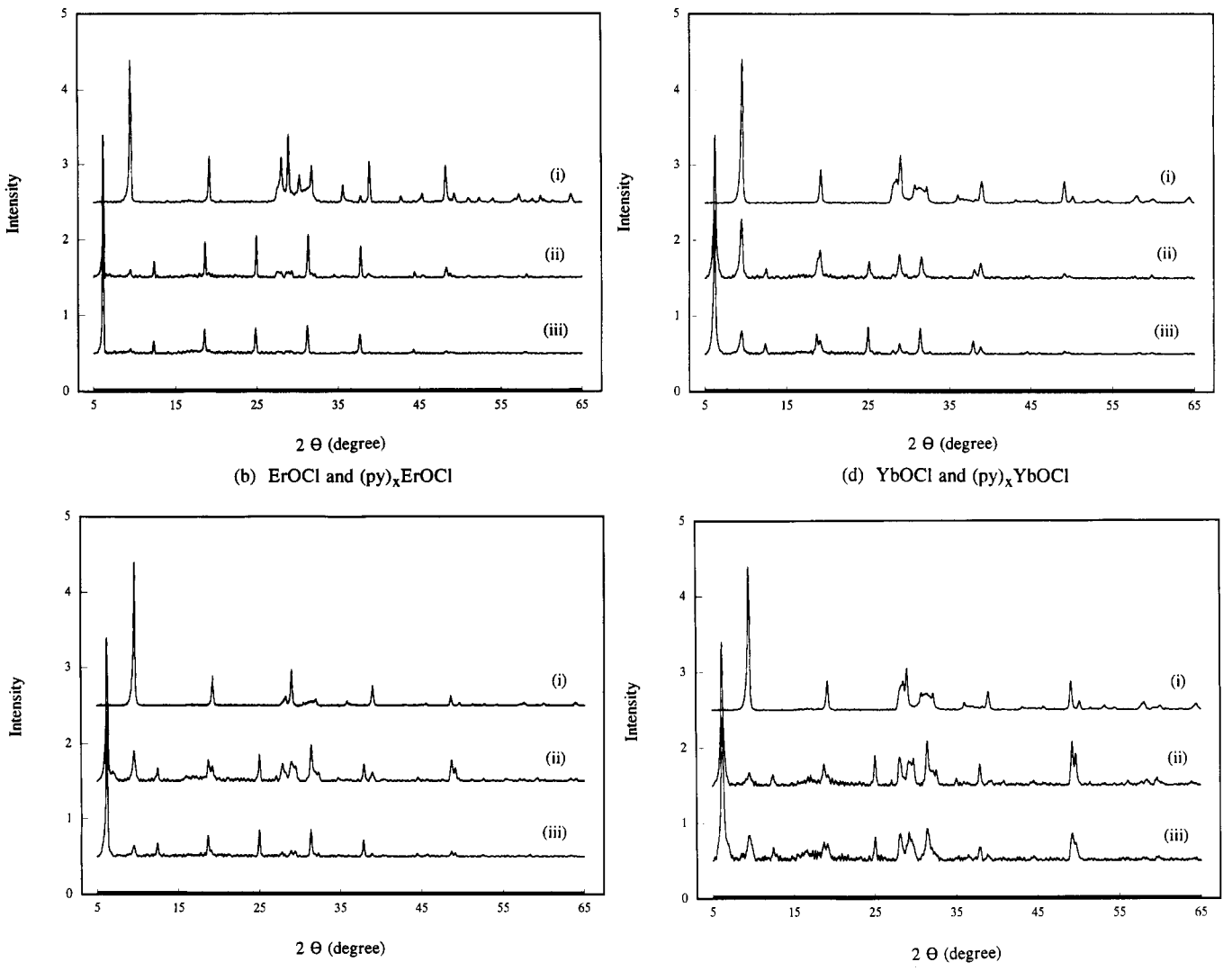

Figure 3. X-ray powder diffraction patterns for (i) LnOCl, and (py)$_x$LnOCl intercalation compounds prepared at (ii) room temperature, 2 weeks and (iii) room temperature, 4 weeks.

Table 2. Stoichiometries of Pyridine (x) and Lattice Parameters and Calculated Interlayer Spacing Changes (Δd) for (py)$_x$LnOCl Compounds Prepared at Room Temperature

compound	x	reaction time (weeks)	a (Å)	c (Å)	Δd (Å)
(py)$_x$HoOCl	0.08	2	3.764 (2)	42.78 (1)	5.00
	0.10	4	3.767 (3)	42.90 (2)	5.04
(py)$_x$ErOCl	0.17	2	3.740 (2)	42.72 (4)	5.00
	0.17	4	3.739 (2)	42.76 (4)	5.01
(py)$_x$TmOCl	0.11	2	3.722 (4)	42.60 (6)	4.96
	0.15	4	3.718 (2)	42.68 (6)	4.99
(py)$_x$YbOCl	0.15	2	3.697 (1)	42.68 (2)	5.00
	0.14	4	3.699 (2)	42.70 (4)	5.01

ature (85 °C) does not significantly change the amount of pyridine that can be intercalated.[27] In the case of (py)$_x$HoOCl and (py)$_x$TmOCl compounds, however, the content of intercalated pyridine (x) reaches the maximum after 4 weeks and is negatively affected by the higher reaction temperature.[27] Although one might expect these compounds to react similarly, their reaction chemistry is obviously different. Since all the hosts are prepared and processed in the same manner there must be other factors that give rise to the differences in reactivity. HoOCl appears to be the most difficult to intercalate, based on the rate and amount of pyridine intercalated. The unintercalated HoOCl is also unusual in that it decomposes at a much lower temperature (~350 °C) compared with the other LnOCl compounds that decompose above 600 °C.

Table 3. Elemental Analysis[a] (wt %) and Calculated Elemental Analysis Based on TGA Data Given in Parentheses

compound	x	C (%)	H (%)	N (%)
(py)$_x$HoOCl		2.87	0.50	0.44
		2.80	<0.50	<0.5
	0.10	(2.68)	(0.22)	(0.62)
(py)$_x$ErOCl		4.79	0.50	0.98
		5.18	0.51	0.60
	0.17	(4.40)	(0.37)	(1.03)
(py)$_x$TmOCl		4.06	0.44	0.78
		4.08	<0.5	0.88
	0.15	(3.88)	(0.33)	(0.90)
(py)$_x$YbOCl		4.26	0.39	0.79
		4.11	<0.50	0.90
	0.14	(3.57)	(0.30)	(0.83)

[a] The first weight percent is from ref 21 and the second weight percent is from ref 23.

Intercalation reactions of the LnOCl with substituted pyridines, 4-ethylpyridine, and 2,6-lutidine, are carried out at room temperature for 2 weeks. Both X-ray powder

Table 4. Interlayer Spacing Changes Obtained from the Shift of (003) Reflections for the Intercalates of Pyridine and Substituted Pyridines Prepared at Room Temperature for 2 Weeks

	Δd (Å)			
intercalant	HoOCl	ErOCl	TmOCl	YbOCl
pyridine	5.0	5.0	4.9	4.9
2,6-lutidine	4.7			
4-ethylpyridine	5.9	6.1	6.8[a]	7.0[a]
			5.4	6.0

[a] Two shifts of the (003) reflections are observed upon intercalation.

diffraction and TGA data are used to characterize the resulting compounds. (4-ethylpyridine)$_x$LnOCl compounds are obtained for all the oxychlorides by reactions of the LnOCl with 4-ethylpyridine. Again, HoOCl reacts differently from the other compounds and is the only host that forms an intercalation compound with 2,6-lutidine (Table 4). Further discussion of the results in Table 4 will be given in regards to the pyridine orientation between the host layers. X-ray powder diffraction patterns of (4-ethylpyridine)$_x$LnOCl and (2,6-lutidine)$_x$HoOCl are provided as supplementary material.

Characterization. Figure 3 shows the X-ray powder diffraction patterns for the LnOCl hosts and their pyridine intercalation compounds, (py)$_x$LnOCl, prepared at room temperature for 2 and 4 weeks. The significant shifts of the reflection peaks from the (00l) lattice planes for all the pyridine intercalates clearly indicate the interlayer expansions of host materials along the c axis upon pyridine intercalation. Preferred orientation leading to increased intensity in the (00l) reflections is also shown in Figure 3. The reflections have been indexed and the lattice parameters for the (py)$_x$LnOCl compounds are provided in Table 2. The interlayer spacing changes (Δd) are obtained from the differences between the c lattice parameters for the hosts and pyridine intercalates and dividing by 3 (to take into account the three layers). Intercalation compounds of (py)$_{0.08}$HoOCl, (py)$_{0.17}$ErOCl, (py)$_{0.11}$TmOCl, and (py)$_{0.15}$YbOCl, prepared at room temperature for 2 weeks, show the interlayer spacing changes of about 5.00 Å. Intercalation compounds prepared at room temperature for 4 weeks, (py)$_{0.10}$HoOCl, (py)$_{0.17}$ErOCl, (py)$_{0.15}$TmOCl, and (py)$_{0.14}$YbOCl, also revealed the interlayer expansions of about 5.00 Å. The resulting interlayer spacing changes of ~5 Å for pyridine intercalated into the LnOCl's are small compared with other layered compounds. For example, Δd's for the LnOCl are much smaller than those observed for pyridine intercalation in the FeOCl (5.35–5.68 Å),[2,8,9] or the transition-metal dichalcogenides (5.80–6.09 Å).[2,4,5] The smallest interlayer spacing change observed for pyridine intercalates in transition metal layered hosts is about 3.3 Å, and it is proposed that the plane of the molecule is oriented parallel to the layers of the host.[12,28]

The pyridine stoichiometries in all the intercalation compounds are obtained from thermal gravimetric analysis (TGA) and elemental analysis and are given in Table 3. Figure 4 shows TGA graphs with the weight loss percentage as a function of temperature for the LnOCl hosts and their pyridine intercalates. Pyridine deintercalates completely from the host layers for all the intercalation compounds by 250 °C, which is indicated by the observation of no subsequent weight loss in the TGA after this temperature and is confirmed by MS data and X-ray powder diffraction. The amount of intercalated pyridine is calculated from the difference in weight percentage between the host and intercalate and is in good agreement with that obtained by elemental analysis. X-ray powder diffraction shows complete recovery of the LnOCl host, with slightly broader reflections. The host material eventually decomposes to Ln_2O_3 after 600 °C as indicated by X-ray powder diffraction with the loss of Cl ions as HCl gas as indicated by MS data. In a study of the thermal decomposition of YOCl, it was also found that the final product is Y_2O_3.[29] Where the hydrogen comes from is uncertain, but it could be due to the presence of small amounts of hydrogen in the deintercalated product. Elemental analysis of the intercalates is consistently high in H content and may be a result of trace amounts of H_2O present in pyridine even after drying and distillation. Although excess H in the elemental analysis may be interpreted as the presence of pyridinium, the intercalates show only a single weight loss in the TGA, implying that there exists only one type of the pyridine species between the host layers. MS also shows the deintercalation of one species in the temperature profile of the selected mass of pyridine for all samples except (py)$_{0.15}$TmOCl, which shows a small shoulder. The shoulder may indicate that there is a different interaction of a small amount of pyridine with the host lattice. This might be interpreted as the presence of a small amount of pyridinium present in the lattice which upon deintercalation undergoes the reaction given below and is subsequently detected as pyridine:

$$pyH^+ + Cl^- \text{ (lattice)} \rightarrow py + H^+\cdots Cl^- \text{ (lattice)}$$

Infrared spectroscopy is used to provide further information about the type of pyridine species, such as neutral pyridine, pyridinium, or dipyridine, present between the host layers. Figure 5 displays infrared spectra for the LnOCl and their pyridine intercalates, (py)$_x$LnOCl, in the range 500–1700 cm^{-1} with a resolution of 2 cm^{-1}. It is shown that all the LnOCl have two adsorptions corresponding to the lanthanide–oxygen vibrations, classified to the A_{2u} and E_u species.[30,31] They occur in 550 and 594 cm^{-1} for HoOCl, 559 and 599 cm^{-1} for ErOCl, 561 and 607 cm^{-1} for TmOCl, and 561 cm^{-1} and 610 cm^{-1} for YbOCl, respectively. The disappearance of the Ln–O (E_u) vibrations in the (py)$_x$LnOCl spectra may be related to interactions between the Ln^{3+} ions in the hosts and pyridine molecules. The infrared adsorptions observed for the intercalated pyridine species as indicated by asterisks are summarized in Table 5, along with the corresponding vibrations. They are found to be compatible with the infrared adsorptions due to neutral pyridine molecules.[9,11,16,32,33] There is no adsorption observed from other pyridine species such as pyridinium (characteristic peak at 1535 cm^{-1})[16,34] or dipyridine,[10] often found in the pyridine interaction compounds of transition-metal disulfides. Even though (py)$_{0.15}$TmOCl shows a small shoul-

(28) Whittingham, M. S. *Mater. Res. Bull.* **1978**, *13*, 775.

(29) Markovskii, L. Y.; Pesina, E. Y.; Omel'chenko, Y. A.; Kondrashev, Y. D. *Russ. J. Inorg. Chem.* **1969**, *14*, 7.

(30) Basile, L. J.; Ferraro, J. R.; Gronert, D. *J. Inorg. Nucl. Chem.* **1971**, *33*, 1047.

(31) Hase, Y.; Dunstan, P. O.; Temperini, M. L. A. *Spectrochim. Acta* **1981**, *37A*, 597.

(32) Thornton, D. A. *Coord. Chem. Rev.* **1990**, *104*, 251.

(33) Johnson, J. W.; Jacobson, A. J.; Brody, J. F.; Rich, S. M. *Inorg. Chem.* **1982**, *21*, 3820.

(34) Gill, N. S.; Nuttall, R. H.; Scaife, D. E.; Sharp, D. W. A. *J. Inorg. Nucl. Chem.* **1961**, *18*, 79.

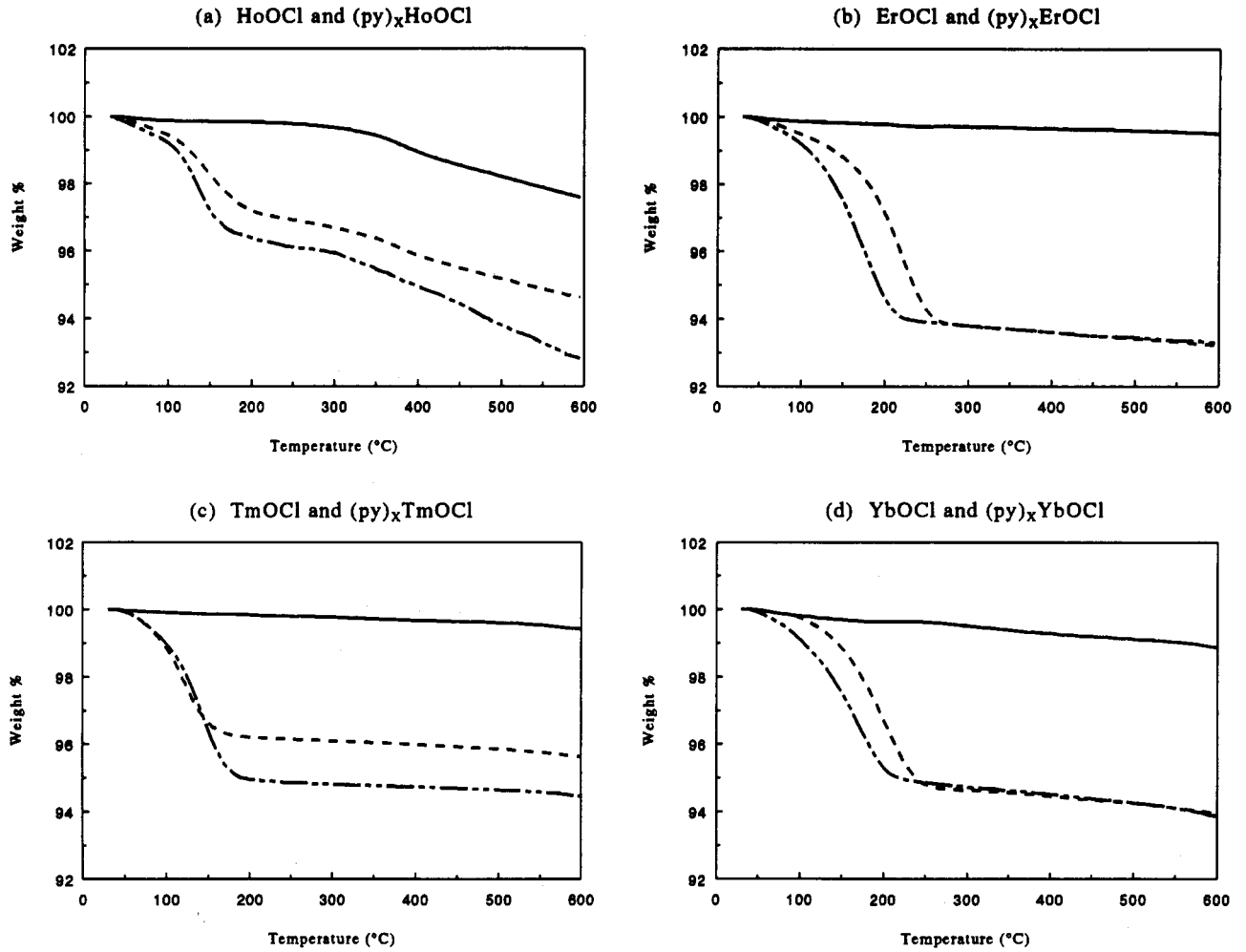

Figure 4. Thermal gravimetric analysis (TGA) curves for (a) HoOCl and $(py)_xHoOCl$, (b) ErOCl and $(py)_xErOCl$, (c) TmOCl and $(py)_xTmOCl$, and (d) YbOCl and $(py)_xYbOCl$, respectively. (—)LnOCl, (- - -) intercalation of pyridine at room temperature for 2 weeks, and (– · · –) intercalation of pyridine at room temperature for 4 weeks.

der in the temperature profile of the selected mass of pyridine, no pyridinium is detected in the IR. If pyridinium is present, it must be a very small amount. We have also explored the reactions of pyridine with LnOCl that has not been rigorously dried, and the IR spectra clearly show the presence of pyridinium.[27]

To verify the lack of reduction of the lanthanide, we obtained magnetic susceptibility data. HoOCl, ErOCl, TmOCl, and YbOCl are all paramagnetic materials due to the unpaired f electrons for the Ho^{3+} (f^{10}), Er^{3+} (f^{11}), Tm^{3+} (f^{12}), and Yb^{3+} (f^{13}) ions. The magnetic susceptibility versus temperature curves for the LnOCl and $(py)_xLnOCl$ are plotted in Figure 6 from 10 to 300 K. The data from 100 K to 300 K were fit to the Curie–Weiss law:

$$\chi_m = C/(T + \theta) + \chi_0$$

χ_0 is the diamagnetic constant showing the temperature independent contribution to the total susceptibility, and C and θ are the Curie and Weiss constants, respectively. The three constants obtained from the hosts and intercalated compounds are listed in Table 6. The effective magnetic moments are calculated from the equation

$$\mu_{eff} = \sqrt{7.99C}\,\mu_B$$

where C is the Curie constant obtained from the fit to the data (100–300 K). The intercalation compounds of $(py)_{0.08}HoOCl$, $(py)_{0.17}ErOCl$, $(py)_{0.11}TmOCl$, and $(py)_{0.15}YbOCl$ have almost the same effective magnetic moments as the unintercalated LnOCl hosts. If there were significant electron transfer from the guest to the host, obvious changes in magnetic susceptibility would be expected, especially for YbOCl whose electron configuration would be expected to change from f^{13} (Yb^{3+}) to closed-shell f^{14} (Yb^{2+}). One would expected to see a decrease in the effective moment for the intercalates of Ho, Er, Tm, and Yb. The magnetic moments show a very slight decrease for Ho, Er, an increase for Yb, and Tm remains unchanged. It is more probable that the slight changes in moment are due to changes in the crystal field rather than reduction of the host lattice. In addition, there are only very small differences in either χ_0 or θ, implying little or no change in the magnetic state of the lanthanide cation.

Mode of Intercalation. On the basis of the above observations, the intercalated pyridine species between the layers of LnOCl are most likely present as neutral pyridine molecules. This suggestion is consistent with the IR data, the observation of single weight loss in the TGA, the single peak in the MS (with the exception of $(py)_{0.15}TmOCl$, which shows a small shoulder), and the magnetic susceptibility data. As a result, a redox mechanism,[2,10,35] which has been proposed for the intercalation of pyridine into the transition-metal disulfides and iron oxychloride due to the observation of the pyridinium and

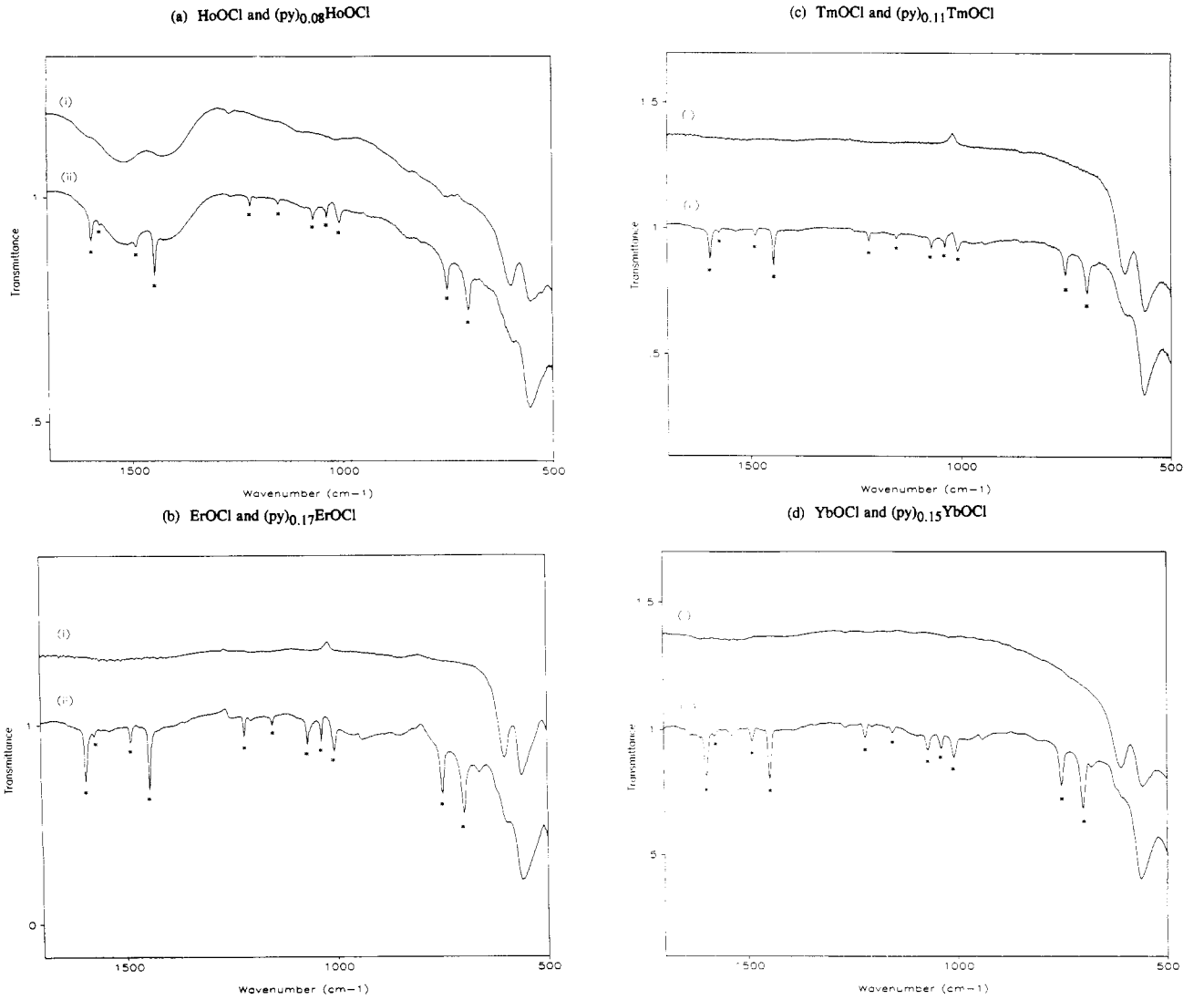

Figure 5. Infrared spectra observed from (i) LnOCl, and (ii) $(py)_xLnOCl$ compounds prepared at room temperature for 2 weeks. Asterisks indicate bands assigned to pyridine.

Table 5. IR Absorption Assignments for Free Pyridine and Intercalated Pyridine in the $(py)_xLnOCl$ Compounds

vibration	pyridine (cm^{-1})	$(py)_{0.08}HoOCl$ (cm^{-1})	$(py)_{0.17}ErOCl$ (cm^{-1})	$(py)_{0.11}TmOCl$ (cm^{-1})	$(py)_{0.15}YbOCl$ (cm^{-1})
ν (ring)	1598	1595	1596	1597	1596
	1582	1575	1576	1577	1576
	1483	1489	1489	1488	1487
	1438	1443	1444	1444	1444
δ (C–H)	1217	1216	1216	1216	1216
	1147	1151	1151	1151	1151
	1069	1069	1068	1068	1068
ν (ring)	1030	1036	1036	1036	1036
	991	1004	1005	1005	1005
γ (C–H)	748	749	749	749	749
	704	698	698	697	698

dipyridine species, is not a suitable mechanism for the pyridine insertion with the LnOCl hosts. In all cases where a redox mechanism has been proposed, in addition to the observation of pyridinium, there are significant changes in the electronic and magnetic properties of the host upon intercalation.[2,6,7,36,37] In the case of the $(py)_xLnOCl$ compounds, there is little or no change in the magnetic properties that can be attributed to a redox mechanism. There is little or no change in color of the material after intercalation with pyridine, whereas alkali metal–ammonia intercalates which must intercalate via a redox mechanism show significant color changes compared to the host.[18,19] In addition, the presence of H_2O in pyridine does not appear to affect either the rate of the reaction or the final stoichiometry of the intercalate.[27] YbOCl is the only LnOCl that might be easily reduced and all the data, including the temperature-dependent magnetic susceptibility indicates that there is no reduction of the Ln^{3+} cation. We have proposed for $(py)_xYbOCl$[20] that a Lewis

(35) Schöllhorn, R.; Zagefka, H. D.; Butz, T.; Lerf, A. *Mater. Res. Bull.* **1979**, *14*, 369.
(36) Whittingham, M. S.; Dines, M. B. *Surv. Prog. Chem.* **1980**, *9*, 55.
(37) Gamble, F. R.; Geballe, T. H. *Treatise Solid State Chem.* **1980**, *3*, 89.

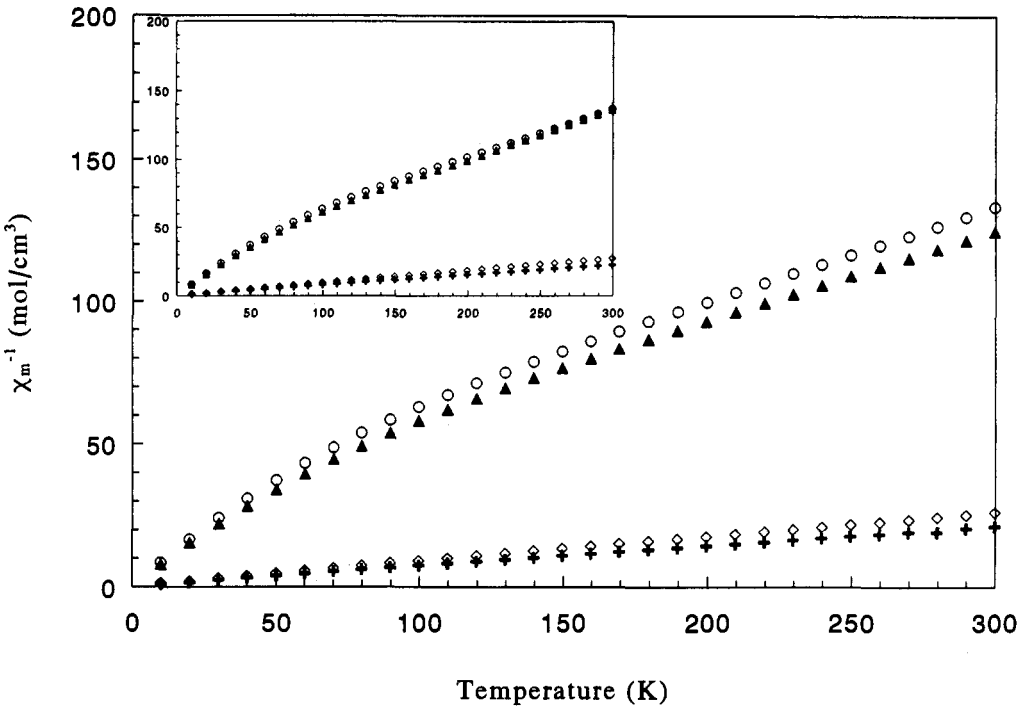

Figure 6. Inverse molar susceptibility versus temperature from 10 to 300 K for the LnOCl hosts and $(py)_xLnOCl$ compounds (inset) + Ho compounds, ◊ Er compounds, ○ Tm compounds, and Δ Yb compounds.

Table 6. Curie–Weiss Parameters and Effective Magnetic Moments Obtained between 100 and 300 K for the Compounds of LnOCl and $(py)_xLnOCl$ (Room Temperature, 2 weeks)

compound	χ_0 (emu/mol)	θ (K)	C (emu K/mol)	μ_{eff} (μ_B)
HoOCl	0.0011 (2)	8.4 (5)	14.15 (7)	10.6 (7)
$(py)_{0.08}$HoOCl	0.0011 (3)	7.5 (9)	13.1 (1)	10.2 (9)
ErOCl	0.0001 (1)	10.3 (5)	11.83 (6)	9.7 (7)
$(py)_{0.17}$ErOCl	0.0006 (2)	8.7 (7)	11.03 (8)	9.4 (8)
TmOCl	0.0012 (1)	53 (3)	2.22 (5)	4.2 (6)
$(py)_{0.11}$TmOCl	0.0010 (1)	54 (4)	2.23 (8)	4.2 (8)
YbOCl	0.0014 (1)	48 (3)	2.31 (5)	4.3 (6)
$(py)_{0.15}$YbOCl	0.0002 (2)	62 (4)	2.58 (9)	4.5 (8)

acid–base mechanism may be more appropriate in explaining the intercalation process. This mode of interaction has also been proposed for Lewis bases intercalated into layered compounds such as MoO_3,[14] $VOPO_4$ and $VOAsO_4$,[33] and V_2O_5.[16] The only other possible mechanism is one that has been proposed recently for the intercalation of pyridine into $MnPS_3$[11] in which the removal of some of the Mn^{2+} ions from the lattice creates vacancies and is solvated by hydroxide ions between the layers. For the LnOCl's, there is no evidence for Ln^{3+} or pyridinium ion in the pyridine supernatant, so it appears that the acid–base mode of interaction best describes the $(py)_xLnOCl$ compounds. A typical adsorption occurring at 1444 cm^{-1} for the base pyridine bound to the acidic metal site[16] is observed in all the intercalates. The fact that infrared absorption bands for the intercalated pyridine at 1005, 1036, 1151, 1444, and 1489 cm^{-1} are shifted to higher frequencies, compared with 991, 1030, 1147, 1438, and 1483 cm^{-1} for free pyridine molecules, is consistent with the proposal that the LnOCl layers behave as a Lewis acid and the pyridine molecules act as the Lewis base.[38]

Pyridine Orientation. The orientation of the pyridine molecules between the layers of the hosts is of considerable interest and aids in understanding the guest–guest and guest–host interactions. Three distinct orientations of pyridine molecules between the layers of the transition

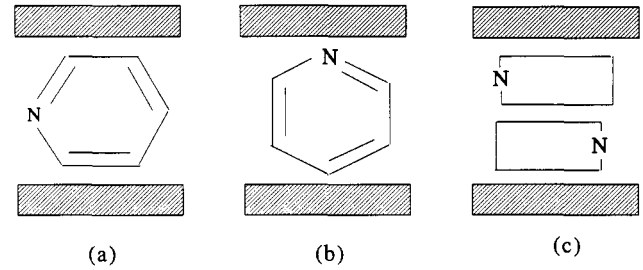

Figure 7. Three orientations of pyridine between the host layers.

metal disulfides have been proposed in Figure 7.[2,28,35] The interlayer spacing increase of ~5.8 Å upon pyridine intercalation has been reported for the orientations indicated in Figure 7a,b. Both orientations display the pyridine ring perpendicular to the host layers. The bilayer arrangement shown in Figure 7c was reported with an interlayer spacing change of ~6.6 Å, since the thickness of pyridine ring is ~3.3 Å. An average of ~5-Å interlayer expansion in the $(py)_xLnOCl$ compounds, as determined by the X-ray powder diffraction data (Table 2), allows us to rule out the orientation with pyridine ring parallel to the host layers as shown in Figure 7c. The small interlayer spacing for the $(py)_xLnOCl$ compounds compared to pyridine intercalates of the transition-metal disulfides may arise from the different intercalation mechanisms proposed for the two systems. The redox mechanism involved in pyridine intercalation of the transition metal disulfides has been shown to be most consistent with the C_2 axis of the pyridine molecule oriented parallel to the layers as shown in Figure 7a. The acid–base interaction between the LnOCl and pyridine requires that the lone-pair electrons of the N atoms on pyridine point toward the host layers as displayed in Figure 7b. For the Δd to be only about 5 Å instead of 5.8 Å, there must be either significant nesting of the pyridine molecules within the

(38) *Spectroscopy and Structures of Molecular Complexes*; Yarwood, J., Ed.; Plenum: New York, 1973; p 281.

host layers, or else the pyridine molecules are inclined slightly with respect to the LnOCl layers.

Studies on the intercalation of the LnOCl with substituted pyridines, 4-ethylpyridine and 2,6-lutidine, aid in ascertaining the pyridine orientation between the layers of the LnOCl. If pyridine is oriented as shown in Figure 7b, one would expect an increase in Δd compared with pyridine when intercalated by 4-ethylpyridine. The X-ray powder diffraction data listed in Table 4 provide the interlayer spacing changes (Δd) obtained from the reflection shifts of the (003) lattice planes for the 4-ethylpyridine intercalates of HoOCl (5.9 Å), ErOCl (6.1 Å), TmOCl (6.8 and 5.4 Å in relative intensity 100 and 26%), and YbOCl (7.0 and 6.0 Å in relative intensity 100 and 57%), respectively. All intercalates show a larger Δd than observed for the pyridine intercalates with YbOCl showing the largest Δd of ~7 Å. Two interlayer spacing changes are observed in the intercalates of TmOCl and YbOCl, indicating different orientations of 4-ethylpyridine between the host layers. Although intercalation of 2,6-lutidine into ErOCl, TmOCl, and YbOCl is unsuccessful, HoOCl shows an interlayer spacing change of 4.7 Å, which is similar to the pyridine intercalates. In comparison with pyridine intercalates, the obvious interlayer spacing increase obtained from 4-ethylpyridine intercalates of all the LnOCl and the little change observed for the 2,6-lutidine intercalate of HoOCl are most consistent with the C_2 axis of pyridine molecule oriented perpendicular to the host layers as shown in Figure 7b.

Summary

A series of new intercalation compounds of the layered lanthanide oxychlorides, LnOCl (Ln = Ho, Er, Tm, and Yb), with pyridine has been successfully obtained at room temperature. The intercalated pyridine stoichiometries (x) in the $(py)_xLnOCl$ compounds, determined by thermal gravimetric analysis (TGA), remain constant after 2 weeks for the $(py)_xErOCl$ and $(py)_xYbOCl$, and reach the maximum after 4 weeks for the $(py)_xHoOCl$ and $(py)_xTmOCl$. The pyridine species inserted between the host layers are most likely neutral pyridine molecules, as determined by TGA, MS, and IR. An acid–base mechanism is proposed for the intercalation of pyridine into the lanthanide oxychlorides, based on the absence of the pyridinium and dipyridine in the IR spectra, the deintercalation of only pyridine in the MS, and the similar magnetic susceptibilities between the LnOCl and $(py)_x$-LnOCl compounds. An average interlayer expansion of ~5 Å between the LnOCl layers upon pyridine intercalation suggests the pyridine ring oriented basically perpendicular to the host layers with either significant nesting or a slight tilt with respect to the layers. In addition, the intercalation reactions of substituted pyridines of 4-ethylpyridine and 2,6-lutidine are most consistent with the C_2 axis of the pyridine molecules being perpendicular to the host layers.

Acknowledgment. We thank Professor R. N. Shelton for the use of the X-ray powder diffractometer and thermogravimetric analyzer, A. Daniel Jones, UC Davis Facility for Advanced Instrumentation, Pingqi Dai for the MS data, and Debra Odink for assistance with preliminary aspects of this work. The work was supported by the donors of the Petroleum Research Fund, administered by the American Chemical Society, and NSF (DMR-9201041).

Supplementary Material Available: Tables of indexed powder diffraction patterns for LnOCl and $(py)_xLnOCl$ (Ln = Ho, Er, Tm, and Yb) and tables and figures of X-ray powder diffraction data for $(4\text{-ethylpyridine})_xLnOCl$ and $(2,6\text{-lutidine})_xHoOCl$ (16 pages). Ordering information is given on any current masthead page.